Detailed Dissection of a New Mechanism for Glycoside Cleavage: α-1,4-Glucan Lyase†

Seung Seo Lee,‡ Shukun Yu,§ and Stephen G. Withers*,‡

Department of Chemistry, University of British Columbia, Vancouver, British Columbia, Canada V6T 1Z1, and Danisco Innovation, Danisco A/S, Langebrogade 1, PO Box 17, DK 1001 Copenhagen K, Denmark.

Received July 8, 2003; Revised Manuscript Received September 1, 2003

ABSTRACT: The unusual enzyme, *Gracilariopsis* α-1,4-glucan lyase of the sequence-related glycoside hydrolase family 31, cleaves the glycosidic bond of α-1,4-glucans via a β-elimination reaction involving a covalent glycosyl−enzyme intermediate (Lee, S. S., Yu, S., and Withers, S. G. (2002) *J. Am. Chem. Soc. 124*, 4948−4949). The classical bell-shaped pH dependence of k_{cat}/K_m indicates two ionizable groups in the active site with apparent pK_a values of 3.05 and 6.66. Brønsted relationships of log k_{cat} versus pK_a and log(k_{cat}/K_m) versus pK_a for a series of aryl glucosides both show a linear monotonic dependence on leaving group pK_a with low β_{lg} values of 0.32 and 0.33, respectively. The combination of these low β_{lg} values with large secondary deuterium kinetic isotope effects ($k_H/k_D = 1.16\sim1.19$) on the first step indicate a glycosylation step with substantial glycosidic bond cleavage and proton donation to the leaving group oxygen at the transition state. Developed oxocarbenium ion character of the transition state is also suggested by the potent inhibition afforded by acarbose and 1-deoxynojirimycin ($K_i = 20$ and 130 nM, respectively) and by the substantial rate reduction afforded by adjacent fluorine substitution. For only one substrate, 5-fluoro-α-D-glucopyranosyl fluoride, was the second elimination step shown to be rate-limiting. The large α-secondary deuterium kinetic isotope effect ($k_H/k_D = 1.23$) at C-1 and the small primary deuterium kinetic isotope effect ($k_H/k_D = 1.92$) at C-2 confirm an E2 mechanism with strong E1 character for this second step. This considerable structural and mechanistic similarity with retaining α-glucosidases is clear evidence for the evolution of an enzyme mechanism within the family.

There are many ways for enzymes to break a glycosidic bond, the most common being the hydrolytic process adopted by glycosidases. This abundant pool of enzymes has been the subject of countless mechanistic studies (*1*−*3*), and these analyses have been greatly assisted by the classification of glycosidases into glycoside hydrolase families based on amino acid sequence comparisons, allowing structural and mechanistic prediction of enzyme action (*4*−*6*).

Another way of breaking a glycosidic bond, which involves a β-elimination reaction, is carried out by a group of enzymes known as lyases. Polysaccharide lyases are well-known enzymes that cleave polysaccharides containing uronic acids or their esters (refs *7* and *8* and references therein). These enzymes perform a β-elimination by abstracting the 5-proton, which is activated by the adjacent carboxylic acid group (Scheme 1a) and eliminating the sugar substituent attached to the 4-hydroxyl. These polysaccharide lyases have also been classified according to their amino acid sequences (http://afmb.cnrs-mrs.fr/CAZY/index.htm) but have been the subject of very few mechanistic studies. However, the recent introduction of defined substrates has allowed some insights (*8*). A new class of polysaccharide lyases that work via a completely different mechanism was recently described (*9*−*13*). These are the α-1,4-glucan lyases (EC 4.2.2.13, GLase)[1] that degrade α-1,4-glucans and maltooligosaccharides via a non-hydrolytic, β-elimination process. Unlike polysaccharide lyases, their substrates are non-uronic acid containing glycosides (Scheme 1b). GLase activity has

Scheme 1: Reactions Catalyzed by a Polysaccharide Lyase (A) and an α-1,-4-Glucan Lyase (B)

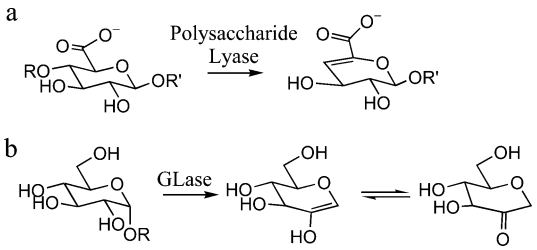

† Authors thank the Natural Sciences and Engineering Council of Canada for financial support. S.S.L. is the holder of the University of British Columbia Graduate Fellowship.

* To whom correspondence should be addressed. Tel: (604) 822-3402. Fax: (604) 822-8869. E-mail: withers@chem.ubc.ca.

‡ University of British Columbia.

§ Danisco Innovation.

[1] Abbreviations: GLase, α-1,4-glucan lyase; 2,4DNPαGlc, 2,4-dinitrophenyl α-D-glucopyranoside; 2,5DNPαGlc, 2,5-dinitrophenyl α-D-glucopyranoside; 3,4DNPαGlc, 3,4-dinitrophenyl α-D-glucopyranoside; 2,4,6TCPαGlc, 2,4,6-trichlorophenyl α-D-glucopyranoside; 4C2NPαGlc, 4-chloro-2-nitrophenyl α-D-glucopyranoside; PNPαGlc, *p*-nitrophenyl α-D-glucopyranoside; ONPαGlc, *o*-nitrophenyl α-D-glucopyranoside; 3,5DCPαGlc, 3,5-dichlorophenyl α-D-glucopyranoside; MNPαGlc, *m*-nitrophenyl α-D-glucopyranoside; PCPαGlc, *p*-chlorophenyl α-D-glucopyranoside; PαGlc, phenyl α-D-glucopyranoside; αGlcF, α-D-glucopyranosyl fluoride; 5FαGlcF, 5-fluoro-α-D-glucopyranosyl fluoride; 2FαGlcF, 2-deoxy-2-fluoro-α-D-glucopyranosyl fluoride; 1FGlcF, 1-fluoro-D-glucopyranosyl fluoride; LC, liquid chromatography; ESI MS, electrospray ionization mass spectrometry; KIE, kinetic isotope effect.

10.1021/bi035189g CCC: $25.00
Published on Web 10/15/2003

		*	
Sugar beet α-glucosidase	460	ILPIDGIWID<u>M</u>NEASNFI	477
Barley high pI α-glucosidase	428	TIPVDGLWID<u>M</u>NEISNFY	445
Spinach α-glucosidase	456	LLPVDGLWID<u>M</u>NEISNFI	473
Human sucrase	1385	KMKFDGLWID<u>M</u>NEPSSFV	1402
Human isomaltase	496	EVQYDGLWID<u>M</u>NEVSSFI	514
Human maltase	520	QVEPDGIWID<u>M</u>NEVSNFV	537
Human lysosomal α-glucosidase	509	QVPFDGMWID<u>M</u>NEPSNFI	526
S. occidentalis glucoamylase	461	LTPFDGIWA<u>D</u>MNEVSSFV	478
Mouse α-glucosidase II α subunit	555	SAPNLYVWN<u>D</u>MNEPSVFN	572
Human α-glucosidase II	532	SAPNLFVWN<u>D</u>MNEPSVFN	549
A. niger α-glucosidase P2 subunit	215	KVAFDGVWY<u>D</u>MSEVSSFV	232
Gracilariopsis α-1,4-glucan lyase	544	SIGLDFVWQ<u>D</u>MTVPAMMP	561
M. costata α-1,4-glucan lyase	539	DMGLEFVWQ<u>D</u>MTTPAIHT	556

FIGURE 1: Partial sequence alignment of selected family 31 α-glucosidases and α-1,4-glucan lyases. Underlined Asp residues are the proposed catalytic nucleophile. Accession numbers are as follows: sugar beet α-glucosidase (Swiss-Prot O04931), barley high pI α-glucosidase (GenBank AF118226), spinach α-glucosidase (Swiss-Prot O04893), human sucrase-isomaltase (Swiss-Prot P14410), human maltase (Swiss-Prot O43451), human lysosomal α-glucosidase (Swiss-Prot P10253), *Schwanniomyces occidentalis* glucoamylase (Swiss-Prot P22861), mouse α-glucosidase II (Swiss-Prot O08794), human α-glucosidase II (GenBank D42041), *Aspergillus niger* α-glucosidase (Swiss-Prot P56526), *Gracilariopsis* sp. α-1,4-glucan lyase (Swiss-Prot P81676), and *Morchella costata* α-1,4-glucan lyase (Swiss-Prot P81696).

been found widely in organisms such as the red algae *Gracilariopsis*, the fungus *Morchella*, *Escherichia coli*, and rat liver (*9*, *14*, *15*), which led to the suggestion of a third pathway of glycogen metabolism (*9*, *15*). Since its isolation in 1993 (*10*), very few studies on α-glucan lyase have been performed beyond the determination of its full amino acid sequence (*9*, *16*, *17*). However, this enzyme is mechanistically interesting in two ways. First, the mechanism of α-1,4-glucan lyase must be different from that of those polysaccharide lyases that cleave the bond between C4 and O1′ of uronic acid-containing polymers to generate a double bond between C4 and C5 of the reducing end sugar. That mechanism relies upon the increased acidity of H-5 resulting from the C-6 carboxyl group. GLases work on simple α-1,4-glucans and cleave the bond between C1′ and O1′, generating a double bond between C1′ and C2′ of the nonreducing end sugar (Scheme 1) without the benefit of an inherently acidic proton. Second, full amino acid sequence alignment reveals significant similarity (23∼28%) with retaining α-glucosidases from glycoside hydrolase family 31 (*9*), with complete conservation of the residue previously identified as the nucleophile in these glycosidases (Figure 1).

Some limited mechanistic data have also been acquired in support of the notion of similarity in the mode of action of α-1,4-glucan lyases and α-glucosidases. Inhibitors of α-glucosidases such as 1-deoxynojirimycin also inhibit GLases (*9*), indicating some similarity in active site structure and therefore also the mechanism (*18*). Carboxyl group-specific inactivators, carbodiimides, have been shown to inactivate GLase (*19*, *20*), implying the involvement of such groups in the mechanism, just as is the case for the α-glucosidases (*2*, *3*). Retaining α-glycosidases (Scheme 2) carry out a two-step mechanism in which a covalent glycosyl−enzyme intermediate is formed and hydrolyzed via oxocarbenium ion-like transition states. One carboxyl group acts as a catalytic nucleophile, forming the covalent glycosyl−enzyme intermediate, while the other acts as a general

Scheme 2: Proposed Mechanism of Retaining Glycosidases

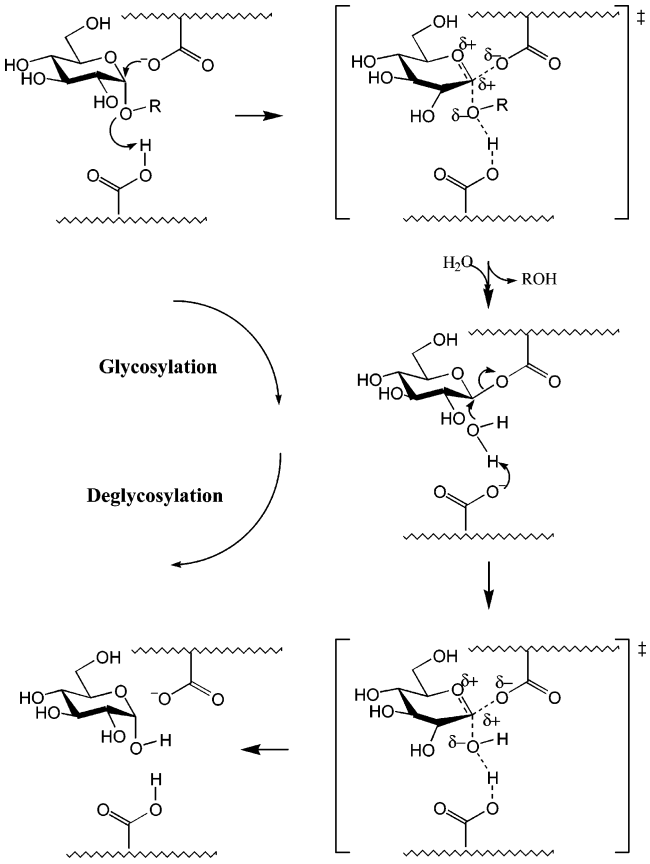

acid catalyst in the first step, donating a proton to the aglycon leaving group and, then as a general base in the second step, removing the proton from the incoming water nucleophile (*1*−*3*). Several family 31 α-glucosidases have been characterized and proven to follow the double displacement mechanism, as evidenced by trapping of the covalent glycosyl−enzyme intermediate (*21*−*25*). These results might suggest that a covalent intermediate is formed on the GLase, despite the appeal of a direct trans-elimination mechanism. In a recent preliminary account (*26*), a covalent glycosyl−enzyme intermediate was trapped on GLase by use of a mechanism-based inactivator of α-glucosidases, a 5-fluoroglycosyl fluoride, and the amino acid residue labeled by this 5-fluorosugar was identified as the same conserved aspartic acid residue that was labeled in the family 31 α-glucosidases. A large α-deuterium kinetic isotope effect on the GLase reaction indicated that, as with family 31 α-glucosidases (*27*, *28*), the reaction proceeds via an oxocarbenium ion-like transition state. Taken together with β-secondary kinetic isotope effect measurements, the results suggest that GLase follows a double displacement mechanism involving the formation of a covalent β-glycosyl−enzyme intermediate, followed by β-elimination of the intermediate, with both steps proceeding via oxocarbenium ion-like transition states.

In this paper, a detailed mechanistic analysis of the α-1,4-glucan lyase from *Gracilariopsis* is provided involving measurements of pH-dependence, Brønsted relationships, kinetic isotope effects, and inhibition studies.

MATERIALS AND METHODS

General Methods. All ^{1}H NMR spectra were recorded at either 200 or 300 MHz using a Bruker AC-200 or AV-300

spectrometer. Mass spectrometry was performed using a PE-Sciex API 300 triple quadrupole mass spectrometer (Sciex, Thornhill, ON, Canada) equipped with an electrospray ionization ion source or performed by the mass spectrometry laboratory at the University of British Columbia. Elemental analysis was performed by the microanalysis laboratory at the University of British Columbia.

Materials. *p*-Nitrophenyl α-D-glucopyranoside, phenyl α-D-glucopyranoside, and D-glucono-1,5-lactone were purchased from Aldrich Chemical Co. 1-Deoxynojirimycin was purchased from Toronto Research Chemicals Inc. (North York, ON, Canada). Acarbose and hydroximinogluconolactam were generous gifts from Miles Inc. (now Bayer) and Dr. Tanja M. Wrodnigg of this laboratory, respectively. 1-Fluoro-D-glucopyranosyl fluoride (refs *29* and *30*, 1FGlcF), 2-deoxy-2-fluoro-α-D-glucopyranosyl fluoride (ref *31*, 2FαGlcF), and 5-fluoro-α-D-glucopyranosyl fluoride (ref *32*, 5FαGlcF) were prepared as previously described. α-D-Glucopyranosyl fluoride (αGlcF) and its 1-[^{2}H] and 2-[^{2}H] derivatives (*33*) and the [1-^{2}H]- and [2-^{2}H]-5-fluoro-α-D-glucopyranosyl fluorides were also synthesized according to published methods (*32*) with the exception that deutero-substrates were synthesized from the corresponding [1-^{2}H]-D-glucopyranose or [2-^{2}H]-D-glucopyranose. [1-^{2}H]-D-Glucopyranose and [2-^{2}H]-D-glucopyranose were purchased from Cambridge Isotope Laboratories, Inc. (Andover, MA). α-1,4-Glucan lyase from *Gracilariopsis* was isolated according to published procedures (*10*, *16*). Pepsin (from porcine mucosa) was purchased from Boehringer Mannheim (Mannheim, Germany). All other chemicals and reagents were purchased from Sigma/Aldrich unless otherwise noted.

Synthesis of Aryl Glucosides. 1,2,3,4,6-Penta-*O*-acetyl-D-glucopyranose (*34*) was used for all syntheses. All solvents were freshly distilled except dimethylformamide (DMF) and chloroform, which were dried extensively over 4 Å molecular sieves. Column chromatography was performed on 230∼400 mesh silica gel (Silicycle, Quebec, Canada). 2,4-Dinitrophenyl 2,3,4,6-tetra-*O*-acetyl-α-D-glucopyranoside (*35*), *p*-chlorophenyl α-D-glucopyranoside (ref *36*, PCPαGlc), and *o*-nitrophenyl α-D-glucopyranoside (ref *37*, ONPαGlc) were prepared as previously described.

BF_3-Diethyl Etherate-Catalyzed Synthesis. This method was a modification of the known procedure (*36*) and was used for synthesizing aryl glucosides formed from phenols without an ortho-nitro substituent. Under a nitrogen atmosphere, boron trifluoride-diethyl etherate (BF_3-OEt_2, 7.63 g, 0.054 mol = 6 equiv) was added to a mixture of 2,3,4,6-tetra-*O*-acetyl-α-D-glucopyranosyl fluoride (3.2 g, 0.009 mol) and the desired phenol (0.4 equiv). The mixture was stirred for 3 h at room temperature, and then saturated $NaHCO_3$ (60 mL) was added. The organic layer was extracted with ethyl acetate (60 mL × 2), washed with water (150 mL) and saturated NaCl (150 mL), dried over $MgSO_4$, and concentrated under vacuum, and the product was purified by column chromatography.

3,4-Dinitrophenyl 2,3,4,6-Tetra-O-acetyl-α-D-glucopyranoside. Purification by column chromatography (97:3 chloroform/acetone, R_f 0.24) and crystallization from diethyl ether yielded white yellowish plates (52%): mp 167 °C, ^{1}H NMR ($CDCl_3$, 300 MHz) δ 8.03 (d, 1 H, $J_{5',6'}$ 9.1 Hz, H5′), 7.52 (d, 1 H, $J_{2',6'}$ 2.5 Hz, H2′), 7.38 (dd, 1 H, $J_{2',6'}$ 2.5, $J_{5',6'}$ 9.1 Hz, H6′), 5.85 (d, 1 H, $J_{1,2}$ 3.7 Hz, H1), 5.63 (dd, 1 H, $J_{2,3}$ 10.4, $J_{3,4}$ 9.8 Hz, H3), 5.14 (dd, 1 H, $J_{3,4}$ 9.8, $J_{4,5}$ 10.3 Hz, H4), 5.07 (dd, 1 H, $J_{2,3}$ 10.4, $J_{1,2}$ 3.7 Hz, H2), 4.20 (dd, 1 H, $J_{5,6a}$ 5.1, $J_{6a,6b}$ 12.4 Hz, H6a), 4.02 (dd, 1 H, $J_{5,6b}$ 2.2, $J_{6a,6b}$ 12.4 Hz, H6b), 3.97 (ddd, 1 H, $J_{4,5}$ 10.3, $J_{5,6a}$ 5.11, $J_{5,6b}$ 2.2 Hz, H5), 2.02∼2.07 (4s, 12 H, 4CH_3s). Anal. Calcd for $C_{20}H_{22}N_2O_{14}$: C, 46.70; H, 4.31; N, 5.45. Found: C, 47.05; H, 4.39; N, 5.83.

3,5-Dichlorophenyl 2,3,4,6-Tetra-O-acetyl-α-glucopyranoside. Purification by column chromatography (97:3 chloroform/acetone, R_f 0.48) yielded a white solid upon the evaporation of solvent (76%): mp 113.5∼114.5 °C, ^{1}H NMR ($CDCl_3$, 300 MHz) δ 7.06 (dd, 1 H, *J* 1.8 Hz, H4′), 7.02 (d, 2 H, *J* 1.8 Hz, H2′, H6′), 5.67 (d, 1 H, $J_{1,2}$ 3.6 Hz, H1), 5.60 (dd, 1 H, $J_{2,3}$ 10.0, $J_{3,4}$ 9.6 Hz, H3), 5.10 (dd, 1 H, $J_{3,4}$ 9.6, $J_{4,5}$ 9.9 Hz, H4), 5.00 (dd, 1 H, $J_{1,2}$ 3.64, $J_{2,3}$ 10.0 Hz, H2), 4.24 (dd, 1 H, $J_{5,6a}$ 6.0, $J_{6a,6b}$ 12.8 Hz, H6a), 4.00∼4.06 (m, 2 H, H5, H6b), 2.02∼2.06 (4s, 12 H, 4CH_3s). Anal. Calcd for $C_{20}H_{22}O_{10}Cl_2$: C, 48.69; H, 4.49. Found: C, 48.62; H, 4.42.

3-Nitrophenyl 2,3,4,6-Tetra-O-acetyl-α-glucopyranoside. Purification by column chromatography (96:4 chloroform/acetone, R_f 0.44) and crystallization from ethyl acetate/hexanes yielded short white needles (45%): mp 101∼102 °C, ^{1}H NMR ($CDCl_3$, 300 MHz) δ 7.92∼7.97 (m, 2 H, H2′, H4′), 7.40∼7.49 (m, 2 H, H5′, H6′), 5.79 (d, 1 H, $J_{1,2}$ 3.6 Hz, H1), 5.67 (dd, 1 H, $J_{2,3}$ 9.9, $J_{3,4}$ 9.8 Hz, H3), 5.15 (dd, 1 H, $J_{3,4}$ 9.8, $J_{4,5}$ 9.7 Hz, H4), 5.05 (dd, 1 H, $J_{1,2}$ 3.6, $J_{2,3}$ 9.9 Hz, H2), 4.23 (dd, 1 H, $J_{5,6a}$ 4.9, $J_{6a,6b}$ 12.2 Hz, H6a), 4.07 (ddd, 1 H, $J_{4,5}$ 9.7, $J_{5,6a}$ 4.9, $J_{5,6b}$ 2.1 Hz, H5), 4.03 (dd, 1 H, $J_{5,6b}$ 2.1, $J_{6a,6b}$ 12.2 Hz, H6b), 2.02∼2.06 (4s, 12 H, 4CH_3s). Anal. Calcd for $C_{20}H_{23}NO_{12}$: C, 51.18; H, 4.94; N, 2.98. Found: C, 51.21; H, 4.77; N, 3.16.

Direct Displacement Reaction at the Anomeric Center. A modification of the published procedure for the synthesis of ONPαGlc (*37*) involving direct displacement of chloride at the anomeric center by the desired phenolate was employed for all aglycones with an ortho-nitro substituent. Under a nitrogen atmosphere, 2,3,4,6-tetra-*O*-acetyl-*β*-D-glucopyranosyl chloride (2.9 g, 0.008 mol) prepared from per-*O*-acetylated glucose by using dichloromethyl methyl ether and boron trifluoride (*38*) was added to a solution of 1,3-dimethyl-3,4,5,6-tetrahydro-2(1*H*)-pyrimidinone (DMPU, 30 mL) containing the sodium salt of the desired phenol (3 equiv) prepared in situ from the phenol and sodium hydride. The solution was stirred for 6 h at 40 °C, then overnight at room temperature. An ice−water mixture (100 mL) was added, and the precipitate was filtered with Celite, washed with water, and then dissolved in methylene chloride (100 mL). The organic layer was washed with $NaHCO_3$ (150 mL), water (150 mL), and saturated NaCl (150 mL) and dried, and then the solvent was evaporated under vacuum.

2,5-Dinitrophenyl 2,3,4,6-Tetra-O-acetyl-α-D-glucopyranoside. Product was purified by column chromatography (97:3 chloroform/acetone, R_f 0.4) and triturated in 1:1 ethyl acetate/hexanes followed by crystallization from diethyl ether as yellowish short needles (11%): mp 134∼136 °C, ^{1}H NMR ($CDCl_3$, 300 MHz) δ 8.25 (d, 1 H, $J_{4',6'}$ 2.2 Hz, H6′), 8.06 (dd, 1 H, $J_{3',4'}$ 8.8, $J_{4',6'}$ 2.2 Hz, H4′), 7.92 (d, 1 H, $J_{3',4'}$ 8.8 Hz, H3′), 5.92 (d, 1 H, $J_{1,2}$ 3.7 Hz, H1), 5.58 (dd, 1 H, $J_{2,3}$ 10.3, $J_{3,4}$ 9.8 Hz, H3), 5.14 (dd, 1 H, $J_{3,4}$ 9.8, $J_{4,5}$ 9.7 Hz, H4), 5.02 (dd, 1 H, $J_{1,2}$ 3.7, $J_{2,3}$ 10.3 Hz, H2), 4.27 (dd, 1 H, $J_{5,6a}$ 5.5, $J_{6a,6b}$ 12.1 Hz, H6a), 4.18 (ddd, 1 H, $J_{4,5}$ 9.7, $J_{5,6a}$

5.5, $J_{5,6b}$ 1.5 Hz, H5), 4.07 (dd, 1 H, $J_{5,6b}$ 1.5, $J_{6a,6b}$ 12.1 Hz, H6b), 2.03∼2.09 (4s, 12 H, $4CH_3$s). Anal. Calcd for $C_{20}H_{22}N_2O_{14}$: C, 46.70; H, 4.31; N, 5.45. Found: C, 46.79; H, 4.30; N, 5.80.

*2,4,6-Trichlorophenyl 2,3,4,6-Tetra-O-acetyl-*α*-*D*-glucopyranoside.* The direct displacement method was employed nicely in this case. Column chromatography was performed (97:3 chloroform/acetone, R_f 0.35), and the product was crystallized from ethyl acetate/hexanes as a white solid (42%): mp 108∼109 °C, ^{1}H NMR ($CDCl_3$, 300 MHz) δ 7.32 (s, 2 H, H3′, H5′), 5.85 (d, 1 H, $J_{1,2}$ 4.0 Hz, H1), 5.70 (dd, 1 H, $J_{3,4}$ 9.7, $J_{2,3}$ 10.5 Hz, H3), 5.18 (dd, 1 H, $J_{1,2}$ 4.0, $J_{2,3}$ 10.5 Hz, H2), 5.15 (dd, 1 H, $J_{3,4}$ 9.7, $J_{4,5}$ 10.3 Hz, H4), 4.79 (ddd, 1 H, $J_{4,5}$ 10.3, $J_{5,6a}$ 4.0, $J_{5,6b}$ 2.4 Hz, H5), 4.25 (dd, 1 H, $J_{6a,6b}$ 12.5, $J_{5,6a}$ 4.0 Hz, H6a), 4.11 (dd, 1 H, $J_{6a,6b}$ 12.5, $J_{5,6b}$ 2.4 Hz, H6b), 2.02∼2.07 (4s, 12 H, $4CH_3$s). Anal. Calcd for $C_{20}H_{21}O_{10}Cl_3$: C, 45.52; H, 4.01. Found: C, 44.56; H, 3.99.

*4-Chloro-2-nitrophenyl 2,3,4,6-Tetra-O-acetyl-*α*-*D*-glucopyranoside.* Column chromatography was performed (97:3 chloroform/acetone, R_f 0.29), and the product was crystallized from ethyl acetate/hexanes as yellowish white needles (10%): mp 141 °C, ^{1}H NMR ($CDCl_3$, 300 MHz) δ 7.80 (d, 1 H, $J_{3',5'}$ 2.5 Hz, H3′), 7.47 (dd, 1 H, $J_{3',5'}$ 2.5, $J_{5',6'}$ 8.9 Hz, H5′), 7.28 (d, 1 H, $J_{5',6'}$ 8.9 Hz, H6′), 5.80 (d, 1 H, $J_{1,2}$ 3.7, H1), 5.60 (dd, 1 H, $J_{2,3}$ 9.8, $J_{3,4}$ 9.8 Hz, H3), 5.15 (dd, 1 H, $J_{3,4}$ 9.8, $J_{4,5}$ 9.8 Hz, H4), 4.98 (dd, 1 H, $J_{2,3}$ 9.8, $J_{1,2}$ 3.7 Hz, H2), 4.23 (dd, 1 H, $J_{5,6a}$ 4.4, $J_{6a,6b}$ 12.0 Hz, H6a), 4.16 (ddd, 1 H, $J_{4,5}$ 9.8, $J_{5,6a}$ 4.43, $J_{5,6b}$ 1.8 Hz, H5), 4.08 (dd, 1 H, $J_{5,6b}$ 1.8, $J_{6a,6b}$ 12.0 Hz, H6b), 2.03∼2.07 (4s, 12 H, $4CH_3$s). Anal. Calcd for $C_{20}H_{22}NO_{12}Cl$: C, 47.68; H, 4.40; N, 2.78. Found: C, 47.96; H, 4.42; N, 3.00.

Acetyl Chloride-Promoted Deacetylation. This method was used for aryl glucosides with acidic phenols (pK_a < 7). Dried acetyl chloride (10% w/w) was added to a solution of the protected sugar (0.5 g) in dry methanol (90 mL), and the reaction mixture was stirred at 4 °C until TLC analysis indicated a complete reaction. The mixture was then concentrated under vacuum, and the resulting oil was either purified by column chromatography or directly crystallized.

2,4-Dinitrophenyl α-D-*Glucopyranoside (2,4DNP*α*Glc).* Reaction time was limited to 5 h to minimize the formation of a side product (R_f 0.17). The product was purified by column chromatography (25:3:2 ethyl acetate/methanol/acetic acid, R_f 0.36) and then crystallized from methanol/chloroform/hexanes as a pale yellowish solid (74%). mp 100∼112 °C (decomp.), ^{1}H NMR (D_2O, 300 MHz) δ 8.80 (d, 1 H, $J_{3',5'}$ 2.8 Hz, H3′), 8.42 (dd, 1 H, $J_{5',6'}$ 9.4, $J_{3',5'}$ 2.8 Hz, H5′), 7.55 (d, 1 H, $J_{5',6'}$ 9.4 Hz, H6′), 5.96 (d, 1 H, $J_{1,2}$ 3.4 Hz, H1), 3.85 (dd, 1 H, $J_{2,3}$ 9.8, $J_{3,4}$ 9.6 Hz, H3), 3.72 (dd, 1 H, $J_{2,3}$ 9.8, $J_{1,2}$ 3.4 Hz, H2), 3.55∼3.63 (m, 3 H, H5, H6a, H6b), 3.44 (dd, 1 H, $J_{3,4}$ 9.6, $J_{4,5}$ 9.1 Hz, H4), ESI MS $[M + Na]^+$ 369.1. Anal. Calcd for $C_{12}H_{14}N_2O_{10} + 1/2H_2O$: C, 40.57; H, 4.26; N, 7.89. Found: C, 40.92; H, 4.50; N, 7.44.

2,5-Dinitrophenyl α-D-*Glucopyranoside (2,5DNP*α*Glc).* The reaction was performed for 5 h. The product was purified by column chromatography (27:3 ethyl acetate/methanol, R_f 0.37) and crystallized from methanol/chloroform/hexanes as white yellowish needles (67%). mp 149∼150 °C, ^{1}H NMR (D_2O, 300 MHz) δ 8.21 (d, 1 H, $J_{4',6'}$ 2.2 Hz, H6′), 8.03 (d, 1 H, $J_{3',4'}$ 8.9 Hz, H3′), 7.96 (dd, 1 H, $J_{3',4'}$ 8.9, $J_{4',6'}$ 2.2 Hz, H4′), 5.93 (d, 1 H, $J_{1,2}$ 3.4 Hz, H1), 3.83 (dd, 1 H, $J_{2,3}$ 9.8, $J_{3,4}$ 9.8 Hz, H3), 3.72 (dd, 1 H, $J_{1,2}$ 3.4, $J_{2,3}$ 9.8 Hz, H2), 3.60∼3.65 (m, 3 H, H5, H6a, H6b), 3.43 (dd, 1 H, $J_{3,4}$ 9.8, $J_{4,5}$ 9.7 Hz, H4), ESI MS $[M + Na]^+$ 369.1. Anal. Calcd for $C_{12}H_{14}N_2O_{10} + 1/2H_2O$: C, 40.57; H, 4.26; N, 7.89. Found: C, 40.73; H, 4.07; N, 7.83.

3,4-Dinitrophenyl α-D-*Glucopyranoside (3,4DNP*α*Glc).* The reaction was performed for 5 h. The product was purified by column chromatography (27:3 ethyl acetate/methanol, R_f 0.26) and crystallized from methanol/chloroform/hexanes as white plates (65%). mp 87∼89 °C, ^{1}H NMR (D_2O, 300 MHz) δ 8.06 (d, 1 H, $J_{5',6'}$ 9.1 Hz, H5′), 7.62 (d, 1 H, $J_{2',6'}$ 2.5 Hz, H2′), 7.42 (dd, 1 H, $J_{2',6'}$ 2.5 Hz, $J_{5',6'}$ 9.1 Hz, H6′), 5.74 (d, 1 H, $J_{1,2}$ 3.5 Hz, H1), 3.81 (dd, 1 H, $J_{3,4}$ 9.3, $J_{2,3}$ 9.9 Hz, H3), 3.68 (dd, 1 H, $J_{2,3}$ 9.9, $J_{1,2}$ 3.5 Hz, H2), 3.50∼3.60 (m, 3 H, H5, H6a, H6b), 3.42 (dd, 1 H, $J_{3,4}$ 9.3, $J_{4,5}$ 9.5 Hz, H4), ESI MS $[M + Na]^+$ 369.1. Anal. Calcd for $C_{12}H_{14}N_2O_{10} + 1/2H_2O$: C, 40.57; H, 4.26; N, 7.89. Found: C, 40.70; H, 4.33; N, 7.79.

4-Chloro-2-nitrophenyl α-D-*Glucopyranoside (4C2NP*α*Glc).* Reaction time was 24 h. Column chromatography was performed with 26:4 ethyl acetate/methanol (R_f 0.20), and the product was crystallized from methanol/chloroform/hexanes as white yellowish plates (46%). mp 96.5∼97 °C, ^{1}H NMR (D_2O, 300 MHz) δ 7.90 (d, 1 H, $J_{3',5'}$ 2.6 Hz, H3′), 7.55 (dd, 1 H, $J_{3',5'}$ 2.6, $J_{5',6'}$ 9.1 Hz, H5′), 7.33 (d, 1 H, $J_{5',6'}$ 9.1 Hz, H6′), 5.78 (d, 1 H, $J_{1,2}$ 3.5 Hz, H1), 3.82 (dd, 1 H, $J_{2,3}$ 9.6, $J_{3,4}$ 9.2 Hz, H3), 3.55∼3.67 (m, 4 H, H2, H5, H6a, H6b), 3.40 (dd, 1 H, $J_{3,4}$ 9.2, $J_{4,5}$ 9.2 Hz, H4). Anal. Calcd for $C_{12}H_{14}NO_8Cl$: C, 42.94; H, 4.20; N, 4.17. Found: C, 42.54; H, 4.59; N, 4.18.

Ammonia-Promoted Deacetylation. This method was used for deacetylating aryl glucosides with relatively basic phenols (pK_a > 7). The protected sugar (0.5 g) was dissolved in dry methanol (30 mL) and cooled on ice, and anhydrous ammonia was bubbled through until the solution was saturated with ammonia (typically 5 min). The reaction mixture was warmed to room temperature, stirred until the reaction was completed, and then concentrated under vacuum.

2,4,6-Trichlorophenyl α-D-*Glucopyranoside (TCP*α*Glc).* The reaction time was 1.5 h, TLC was carried out in 27:3 ethyl acetate/methanol (R_f 0.24), and the product was directly crystallized from methanol as white needles (85%). mp 168 °C, ^{1}H NMR (CD_3OD, 300 MHz) δ 7.40 (s, 2 H, H3′, H5′), 5.90 (d, 1 H, $J_{1,2}$ 3.9 Hz, H1), 4.2 (ddd, 1 H, $J_{4,5}$ 10.0, $J_{5,6a}$ 3.2, $J_{5,6b}$ 3.0 Hz, H5), 3.90 (dd, 1 H, $J_{2,3}$ 9.8, $J_{3,4}$ 9.2 Hz, H3), 3.65∼3.75 (m, 2 H, H6a, H6b), 3.60 (dd, 1 H, $J_{1,2}$ 3.9, $J_{2,3}$ 9.8 Hz, H2), 3.47 (dd, 1 H, $J_{3,4}$ 9.2, $J_{4,5}$ 10.0 Hz, H4). Anal. Calcd for $C_{12}H_{13}O_6Cl_3$: C, 40.08; H, 3.64. Found: C, 40.09; H, 3.70.

3,5-Dichlorophenyl α-D-*Glucopyranoside (DCP*α*Glc).* The reaction was performed for 2 h. The final product was purified by column chromatography (27:3 ethyl acetate/methanol, R_f 0.21) and was obtained as a white solid upon the evaporation of solvent (71%). mp 168 °C, ^{1}H NMR (D_2O, 300 MHz) δ 7.08 (dd, 1 H, J 1.6 Hz, H4′), 7.05 (d, 2 H, J 1.6 Hz, H2′, H6′), 5.52 (d, 1 H, $J_{1,2}$ 3.6 Hz, H1), 3.78 (dd, 1 H, $J_{2,3}$ 9.5, $J_{3,4}$ 9.3 Hz, H3), 3.55∼3.64 (m, 4 H, H2, H5, H6a, H6b), 3.39 (dd, 1 H, $J_{3,4}$ 9.3, $J_{4,5}$ 9.6 Hz, H4). Anal. Calcd for $C_{12}H_{14}O_6Cl_2$: C, 44.33; H, 4.34. Found: C, 44.55; H, 4.42.

3m-Nitrophenyl α-D-*Glucopyranoside (MNP*α*Glc).* The reaction was performed for 2 h. The product was purified

Table 1: Michaelis−Menten Parameters for the Cleavage of a Series of Aryl α-Glucosides by *Gracilariopsis* α-1,4-Glucan Lyase

substrate	pK_a	k_{cat} (s^{-1})[a]	K_m (mM)[a]	k_{cat}/K_m ($s^{-1}\,M^{-1}$)	$\Delta\epsilon$[b] ($mM^{-1}\,cm^{-1}$)
2,4DNPαGlc	3.96	27	3.8	7100	10.3
2,5DNPαGlc	5.15	11	9.9	1100	3.59 (at 440 nm)
3,4DNPαGlc	5.36	1.7	0.59	2900	10.6
2,4,6TCPαGlc	6.39	1.0	0.77	1300	1.60 (at 312 nm)
4C2NPαGlc	6.45	6.3	2.7	2300	0.710 (at 425 nm)
PNPαGlc	7.18	0.40	2.1	190	1.66
ONPαGlc	7.22	5.3	11	480	1.07
3,5DCPαGlc	8.19	1.5	3.1	480	0.726 (at 280 nm)
MNPαGlc	8.39	0.66	2.2	300	0.307 (at 380 nm)
PCPαGlc	9.38	0.44	2.1	210	0.574 (at 278 nm)
PαGlc	9.99	0.11	4.4	25	0.760 (at 277 nm)

[a] Errors in kinetic parameters are less than 10%. [b] $\Delta\epsilon$ values were measured at a wavelength of 400 nm unless otherwise noted.

by crystallization from methanol as short yellowish white needles (78%). mp 183∼184 °C, ^{1}H NMR (D_2O, 300 MHz) δ 7.87∼7.94 (m, 2 H, H2′, H4′), 7.48∼7.51 (m, 2 H, H5′, H6′), 5.70 (d, 1 H, $J_{1,2}$ 3.7 Hz, H1), 3.88 (dd, 1 H, $J_{2,3}$ 9.7, $J_{3,4}$ 9.2 Hz, H3), 3.44∼3.70 (m, 5 H, H2, H4, H5, H6a, H6b). Anal. Calcd for $C_{12}H_{15}NO_8$: C, 47.84; H, 5.02; N, 4.65. Found: C, 48.09; H, 4.95; N, 4.60.

Enzyme Kinetics. All experiments were carried out at 30 °C in 0.1 M MES buffer, pH 6.0 unless otherwise noted.

pH-Dependence Studies. Measurement of the pH-dependent activity of α-1,4-glucan lyase (GLase) was carried out spectrophotometrically at 400 nm using 2,4-dinitrophenyl α-D-glucopyranoside (2,4DNPαGlc) as substrate, using the following buffers: Glycine-HCl (pH 2.42∼3.5), sodium acetate (pH 4.0∼5.5), MES (pH 6.0), MOPS (pH 6.5∼7.5), and Gly-Gly (pH 8). All buffers were 0.05 M and contained 0.05 M NaCl. The substrate-depletion method was employed (*39*). A solution of substrate (0.03 mM, 100-fold lower than the value of K_m) was preincubated at pH 6.0 and 30 °C, and then the release of 2,4-dinitrophenol after the addition of GLase was monitored using a UNICAM UV/VIS spectrophotometer equipped with a circulating water bath until at least 80% depletion of substrate. Cuvettes of 1 or 0.1 cm path length were used. Appropriate controls confirmed that, at 30 °C, GLase is stable. Fitting of the data to a first-order equation (GraFit 4.0, Erithacus Software Ltd., Staines, UK) yielded an apparent rate constant for the reaction, from which k_{cat}/K_m for each substrate was calculated by dividing that rate constant by the concentration of GLase. Obtained k_{cat}/K_m values were then plotted versus pH and fitted to the appropriate curve in GraFit 4.0, yielding apparent pK_a values.

Brønsted Analysis. Michaelis−Menten parameters for the aryl glucosides at 30 °C were measured by monitoring the release of phenols at the appropriate wavelength (Table 1) with a UNICAM UV/VIS spectrophotometer equipped with a circulating water bath. The typical substrate concentration range employed was 0.3∼3 × K_m. The difference in extinction coefficient, $\Delta\epsilon$, between each aryl glucoside and substituted phenol at the relevant wavelength at pH 6.0 and 30 °C was determined by measuring the difference in absorbance between fixed equal concentrations of each pair of phenols and aryl glucosides. Data are presented in Table 1. Kinetic parameters were obtained by direct fit of the data to the Michaelis−Menten equation. Logarithms of obtained kinetic parameters (k_{cat} and k_{cat}/K_m) were fitted linearly with leaving group pK_a values. The Brønsted coefficient, β_{lg}, was obtained from the slope of this plot. All data fitting was performed using GraFit 4.0.

Inhibitor Studies. Inhibition studies were performed by measuring the reduced activity of GLase in the presence of inhibitors, using 2,4DNPαGlc as substrate. GLase (9.8 μg/mL) preincubated at 30 °C was added to 200 μL of buffer solution containing 2,4DNPαGlc and varying amounts of inhibitors, also preincubated at 30 °C. The release of 2,4-dinitrophenol was monitored spectrophotometrically at 400 nm. The experiments were repeated at different concentrations of 2,4DNPαGlc. A Dixon plot of $1/v$ versus inhibitor concentration intersects a line given by $1/V_{max}$ at an inhibitor concentration equal to $-K_i$.

Fluorosugar Kinetics. Kinetic parameters with 1FGlcF, 2FαGlcF, and 5FαGlcF were determined as previously described (*25*). Varying concentrations of these substrates were prepared, and in the presence of the desired concentrations of GLase, the release of fluoride was monitored using an Orion 96-09 combination fluoride ion electrode interfaced to a computer running the LoggerPro software (Vernier Software Ltd.). Initial rates were used for the determination of kinetic parameters. For 1FGlcF and 2FαGlcF, no saturation was observed up to a concentration of 100 mM. Therefore, only k_{cat}/K_m values could be obtained from the slope of the initial low concentration part of the plot. $\Delta\Delta G^{\ddagger}$ was calculated according to the equation $\Delta\Delta G^{\ddagger} = RT \ln[(k_{cat}/K_m)_F/(k_{cat}/K_m)_{F2}]$, where $(k_{cat}/K_m)_F$ is determined for αGlcF and $(k_{cat}/K_m)_{F2}$ for either 1FGlcF or 2FαGlcF. Kinetic parameters for 5FαGlcF were determined by fitting the data to the Michaelis−Menten equation. All fitting processes were performed with GraFit 4.0. An apparent reversible inhibition constant, K_i', was determined by measuring rates of hydrolysis of 2,4DNPαGlc in the presence of various concentrations of 5FαGlcF as described.

Inactivation Test. For inactivation kinetics, the enzyme (final concentration 0.21 mg/mL) was preincubated with an appropriate range of concentrations of either 1FGlcF, 2FαGlcF, or 5FαGlcF (5∼50 mM) at 30 °C, and 10 μL aliquots of the sample were withdrawn at time intervals and added to 500 μL of 5 mM 2,4DNPαGlc, each preequilibrated at 30 °C in the UV/VIS spectrometer. Residual enzyme activity at each time interval at each concentration of each fluorosugar was measured in this way.

Kinetic Isotope Effects (KIE). The KIEs for the k_{cat} of [1-^{2}H]-αGlcF and [2-^{2}H]-αGlcF were determined by measuring initial rates of reaction of GLase with each protio- and deutero-substrate (270 mM, K_m = 27.9 mM) by monitoring the release of fluoride as described previously and dividing the rate for the protio-substrate by the rate for the deutero-substrate in each case. Each measurement was repeated at least six times. The KIEs for the k_{cat} of [1-^{2}H]-5FαGlcF and [2-^{2}H]-5FαGlcF were determined likewise, except at a concentration of 80 mM (K_m = 10.7 mM).

Labeling and Proteolysis of GLases. A stock solution of the enzyme (20 μL, 11.89 mg/mL) was incubated with 5FαGlcF (20 μL, 80 mM) at 30 °C for 30 min. The sample was diluted with 0.05 M phosphate buffer (pH 2, 90 μL) and incubated with pepsin (15 μL, 1 mg/mL) for 15 min at room temperature. The sample was then rapidly frozen and analyzed immediately upon thawing. A control sample was

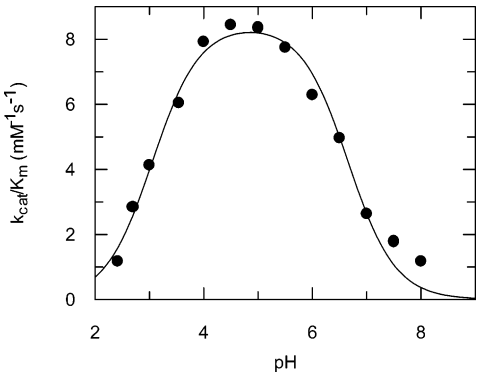

FIGURE 2: pH-Dependence of the cleavage of 2,4DNPαGlc catalyzed by *Gracilariopsis* α-1,4-glucan lyase.

prepared according to the same procedure, except that no 5FαGlcF was added.

Electrospray Mass Spectrometry. Mass spectra were recorded on a PE-Sciex API 300 triple quadrupole mass spectrometer (Sciex, Thornhill, ON, Canada) equipped with an electrospray ionization ion source. Peptides were separated by reverse phase high performance liquid chromatography (HPLC) on an Ultrafast Microprotein Analyzer (Michrom BioResources Inc., Pleasanton, CA) directly interfaced with the mass spectrometer. In each MS experiment, the proteolytic digest was loaded onto a C18 column (Reliasil, 1 × 150 mm) and eluted with a gradient of 0∼60% eluting solvent (0.045% trifluoroacetic acid, 80% acetonitrile in water) over 60 min at a flow rate of 50 μL/min. A postcolumn splitter was used in all experiments, splitting off 85% of the sample into a fraction collector and sending 15% into the mass spectrometer.

The quadrupole mass analyzer was scanned over a *m*/*z* range of 400−2000 Da with a step size of 0.5 Da and a dwell time of 1.0 ms/step. The ion source voltage was set at 5 kV, and the orifice energy was 50 V. After the LC/MS experiment, total ion chromatograms of the labeled and unlabeled enzyme digests were compared to find the fraction containing the labeled peptide fragments.

RESULTS

Measurement of pH-Dependent Activity. To determine the pK_a values of amino acid residues responsible for the activity of free enzyme, k_{cat}/K_m values were measured as a function of pH. The pH−activity profile is shown to be a classical bell-shaped curve, which indicates that there are two essential ionizable groups (Figure 2). Optimum pH was estimated to be pH 4.5, and the two associated pK_a values were 3.05 ± 0.07 and 6.66 ± 0.07.

Measurement of k_{cat} and K_m for Aryl Glycoside Substrates. A series of aryl α-D-glucosides was synthesized to observe the relationship between the kinetic parameters of GLase and the pK_a values of their aglycone leaving groups in the range between pK_a 3.96 and 9.99. All but two commercially available glucosides were made by modifications of published procedures (see Materials and Methods).

Substrates, pK_a values of phenol leaving groups, and kinetic parameters (k_{cat} and K_m) are presented in Table 1. Both k_{cat} and k_{cat}/K_m are only moderately sensitive to the change of pK_a, with k_{cat} values changing only 250-fold from the most to the least reactive substrates.

Table 2: Structure of Inhibitors and K_i Values for *Gracilariopsis* α-1,4-Glucan Lyase

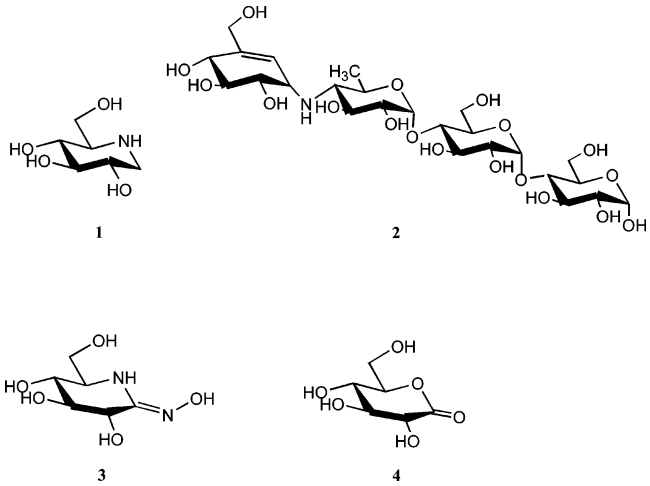

1 **2**

3 **4**

inhibitors	K_i (μM)
1-deoxynojirimycin (**1**)	0.13 ± 0.001
acarbose[a] (**2**)	0.020 ± 0.0003
hydroximinogluconolactam (**3**)	1.3 (± 0.064) × 10^3
D-glucono-1,5-lactone (**4**)	ND[b]

[a] Excerpted from ref *26*. [b] Not detected.

Inhibitors. Although 1-deoxynojirimycin and acarbose were known to inhibit GLase (*9*, *12*), inhibition parameters need to be measured precisely. Thus, along with a few other inhibitors, these were subjected to analysis. Table 2 shows K_i values of the inhibitors tested along with their structures. 1-Deoxynojirimycin and acarbose, which are very potent α-glucosidase inhibitors, proved to be both potent and competitive inhibitors for GLase as well, showing K_i values of 0.13 and 0.020 μM, respectively. Hydroximinogluconolactam (K_i = 1.28 ± 0.06 mM) was shown to be a poor inhibitor. Glucono-1,5-lactone did not inhibit GLase as previously reported (*9*).

Fluorosugar Kinetics. 1-Fluoro-D-glucopyranosyl fluoride (1FGlcF), 2-deoxy-2-fluoro-α-D-glucopyranosyl fluoride (2FαGlcF), and 5-fluoro-α-D-glucopyranosyl fluoride (5FαGlcF) were prepared and tested with GLase. The hope had been that these compounds might act as mechanism-based inactivators and label crucial amino acid residues in the active site. However, when these were incubated with GLase and aliquots were removed at time intervals, no time-dependent inactivation was observed. Rather, the three compounds behaved like slow substrates as was shown by kinetic analysis using the fluoride ion electrode. 1FGlcF and 2FαGlcF bind poorly with high K_m values that could not be measured. Thus, values of k_{cat}/K_m only were measured for these, although values of k_{cat} and K_m could be measured for 5FαGlcF (Table 3). Also given in Table 3 are values of k_{cat} and K_m for α-D-glucopyranosyl fluoride (αGlcF). $\Delta\Delta G^{\ddagger}$ values for 1FGlcF and 2FαGlcF were calculated to reflect the change on the free energy of activation for the first irreversible step (k_{cat}/K_m) as compared to the parent sugar, αGlcF, using the equation $\Delta\Delta G^{\ddagger} = RT \ln[(k_{cat}/K_m)_F/(k_{cat}/K_m)_{F2}]$. The K_m value of 5FαGlcF is substantially lower than that of the parent sugar, αGlcF, and approximately equal to the apparent K_i value determined for 5FαGlcF (K_i') acting as a reversible inhibitor.

Table 3: Michaelis−Menten Parameters for the Cleavage of Fluorosugars by *Gracilariopsis* α-1,4-Glucan Lyase

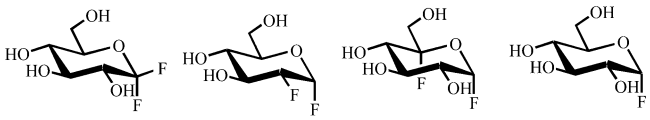

5 **6** **7** **8**

substrate	k_{cat} (s^{-1})[a]	K_m (mM)[a]	k_{cat}/K_m ($s^{-1}\,M^{-1}$)	K_i' (mM)	$\Delta\Delta G^{\ddagger}$ (kJ/mol)
1FGlcF (**5**)			13.8		18.1
2FαGlcF (**6**)			3.81		21.1
5FαGlcF (**7**)	0.131	10.7	12.2	6.48	18.4
αGlcF (**8**)	505	27.9	1.81×10^4		

[a] Errors in kinetic parameters are less than 10%.

Reaction with 5-Fluoro-α-D-glucosyl Fluoride. 5-Fluoro-α-D-glucopyranosyl fluoride and its epimer at the 5-position, 5-fluoro-*β*-L-idopyranosyl fluoride (5F*β*IdoF), are well-established, mechanism-based inactivators for α-glucosidases (*25*, *40*). 5F*β*IdoF was already shown to inactivate GLase in a preliminary communication of this work (*26*) in which the catalytic nucleophile was identified on the basis of MS/MS analysis of a labeled peptide derived from proteolysis of the trapped intermediate. An attempt to inactivate and label GLase with 5FαGlcF was made, but only a small extent of inactivation was observed. The inactivation was not time-dependent within the time scale of the assay. Instead, reduced activity was measured at the shortest time interval possible (30 s) after the mixing of GLase and 5FαGlcF, and this did not change with time. The lower rates presumably arise from reversible inhibition afforded by the 5FαGlcF carried over into the assay mixture—suggesting that 5FαGlcF might be acting as a reversible inhibitor. A Dixon plot was therefore constructed by measuring rates with several concentrations of substrate (2,4-dinitrophenyl α-glucopyranoside) and varying concentrations of 5FαGlcF. The resulting Dixon plot shows that 5FαGlcF acts as an apparent competitive inhibitor with an apparent dissociation constant, K_i', of 6.48 mM (Table 3). The approximate equivalence of this value and its K_m value as a substrate indicates that it is inhibiting by virtue of its reaction as a substrate, possibly via the accumulation of a glycosyl−enzyme intermediate. This would explain why the K_m and K_i' values are lower than that of the parent substrate αGlcF. A number of efforts to detect such a covalent species were made. When GLase previously incubated with 5FαGlcF was loaded onto the microbore RP-HPLC connected to the electrospray ionization mass spectrometer (ESIMS), unfortunately, a full-length protein mass was not detectable. Thus, labeled and unlabeled enzymes were digested by pepsin followed by HPLC/ESI MS analysis. However, a labeled peptide could not be detected under those conditions, either.

Kinetic Isotope Effects (KIEs). Kinetic isotope effects measured for *p*-nitrophenyl α-D-glucopyranoside (PNPαGlc), α-D-glucopyranosyl fluoride, and 5-fluoro-α-D-glucopyranosyl fluoride are presented in Table 4. KIEs upon k_{cat} were measured with PNPαGlc and 5FαGlcF, while KIEs upon both k_{cat} and k_{cat}/K_m, respectively, were measured with αGlcF. Isotope effects arising from deuterium on C-1 and C-2 were measured separately. Data clearly show that all KIEs from the 1-position are large α-secondary KIEs, and values of KIEs from the 2-position of PNPαGlc and αGlcF are close to those of *β*-secondary KIEs, while the magnitude of the KIE from the 2-position of 5FαGlcF falls within the range of a primary effect.

Table 4: Kinetic Isotope Effects Measured for Deuterated Substrates with *Gracilariopsis* α-1,4-Glucan Lyase

substrate	KIE upon k_{cat}	KIE upon k_{cat}/K_m
1-[^{2}H]-PNPαGlc	1.19 ± 0.02[a]	
1-[^{2}H]-αGlcF	1.14 ± 0.05	1.16 ± 0.01[a]
1-[^{2}H]−5FαGlcF	1.23 ± 0.10	
2-[^{2}H]-PNPαGlc	1.06 ± 0.01[a]	
2-[^{2}H]-αGlcF	1.06 ± 0.04	1.07 ± 0.01[a]
2-[^{2}H]−5FαGlcF	1.92 ± 0.15	

[a] Excerpted from ref *26*.

DISCUSSION

The trapping of a covalent glycosyl−enzyme intermediate on GLase, coupled with the earlier dissection of sequence similarities with family 31 α-glucosidases, had suggested mechanistic similarities between the GLase and the retaining α-glucosidases (*9*, *26*). Both mechanisms are therefore thought to be two-step processes involving active site carboxylic acids as acid/base catalysts and as a nucleophile/leaving group with the reaction proceeding via a covalent glycosyl enzyme intermediate. Consistent with this expectation, the pH-dependence of k_{cat}/K_m ($pK_{a1} = 3.05$ and $pK_{a2} = 6.66$) for GLase is very similar to that of the family 31 *Aspergillus niger* α-glucosidase (ref *41*, $pK_{a1} = 3.2$ and $pK_{a2} = 6.4$). Thus, the free enzymes (upon which k_{cat}/K_m reports) have very similar active site environments.

An understanding of the enzymatic transition state structure requires, first, a definition of which step is rate-limiting for any particular substrate. To probe this, the kinetic parameters for a series of aryl glucosides were plotted in the form of Brønsted relationships as shown in Figure 3. These plots of log k_{cat} and log k_{cat}/K_m versus pK_a exhibit a disappointing level of scattering ($R = 0.83$ and 0.90, respectively) but clearly reveal a dependence, albeit shallow ($\beta_{lg} = 0.32$ and 0.33, respectively), of rate on the leaving group ability. The similarity in these slopes suggests that the same step is rate-limiting in the two cases and that this step involves breakage of the aryl glycoside bond. This is reinforced by the fact that k_{cat}/K_m reports on the first irreversible step, which has generally proved to be the formation of the glycosyl−enzyme for retaining glycosidases.

The absence of any break in this plot implies that no change in the rate-limiting step occurs as the leaving group ability increases, as might be expected given that α-glucosyl fluoride has a k_{cat} value of 505 s^{-1}, almost 20 times greater than that of the best aryl glycoside substrate. Interestingly, in no case yet has a biphasic plot been seen for any α-glycosidase, whereas this behavior is quite common for *β*-glycosidases (*3*, *42*, *43*). The low β_{lg} value indicates that relatively little negative charge is present on the glycosidic oxygen at the transition state. Thus, either there is very little glycosidic bond cleavage at the transition state or considerable proton donation has occurred. The former interpretation is rendered unlikely by the measurement of large α-deuterium kinetic isotope effects (Table 4 and ref *26*), which indicate substantial oxocarbenium ion character and thus substantial bond cleavage. Early proton donation therefore seems likely;

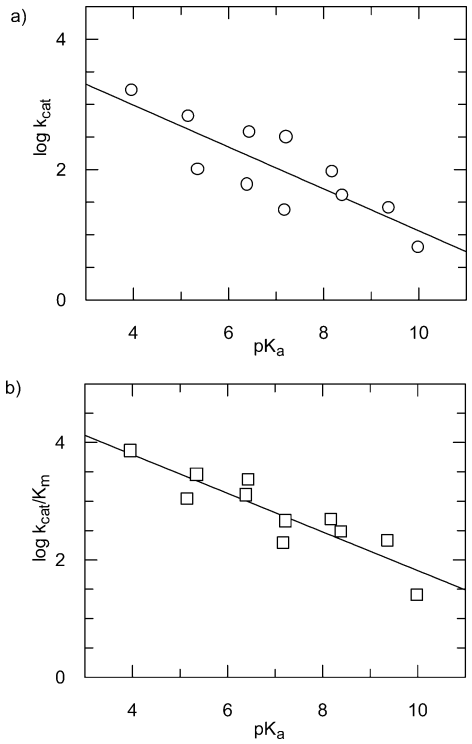

FIGURE 3: Brønsted plot constructed from the data of Table 1 showing the relationship of the rate of cleavage of a series of aryl glucosides with the pK_a of the corresponding phenol. (a) Log k_{cat} vs pK_a and (b) log k_{cat}/K_m vs pK_a.

indeed, similarly low β_{lg} values have been seen with the *Cellulomonas fimi* exoglycanase (*44*) and also with the family 31 sucrase-isomaltase, interpreted likewise (*27*).

Some indications of positively charged transition states are also found in the inhibitor studies performed. The potent competitive inhibition exhibited by acarbose ($K_i = 0.02\ \mu$M), itself a proven transition state analogue inhibitor of family 13 α-glucosidases (*45*), strongly supports reaction via an oxocarbenium ion-like transition state. Likewise, the potent, competitive inhibition by 1-deoxynojirimycin ($K_i = 0.13\ \mu$M) suggests an anionic active site capable of binding positively charged species (*18*). The poor binding affinity of hydroximinogluconolactam ($K_i = 1.3$ mM) is surprising given the high affinity of this compound for family 13 α-glucosidases (*46*). This might imply that family 31 enzymes, for which no three-dimensional structures have yet been reported, are syn protonators, with their acid catalysts sitting in a syn-relationship to the substrate endocyclic C1−O5 bond. Family 13 glycosidases, on the other hand, are known to be anti-protonators. Studies on β-glycosidases have shown that only anti-protonators are significantly inhibited by compounds of this class (*47*, *48*). Poor binding of gluconolactone is less surprising since this is known to be a poor inhibitor of α-glycosidases (*18*).

Kinetic isotope effects provide some of the best probes of transition state structure, and as noted earlier, large α-deuterium kinetic isotope effects were measured previously for the first, glycosylation, step. To probe the transition state structure of the second (elimination) step, it was necessary to identify substrates for which this step is rate-limiting. Unfortunately, none of the aryl glycosides meet this challenge, as shown by the linear Brønsted plot, and even α-glucosyl fluoride, with a k_{cat} value of 505 s^{-1}, appears to have rate-limiting glycosylation as evidenced by the similarity of the deuterium kinetic isotope effects on k_{cat} measured with those measured for PNPαGlc. In an attempt to generate a substrate for which deglycosylation was rate-limiting, attention was turned to modified glycosyl fluorides containing a second fluorine substituent. The best candidate for such a study was 5-fluoro α-glucosyl fluoride (5FαGlcF), the C-5 epimer of the analogue used to trap the covalent intermediate previously. Kinetic analysis (Table 3) revealed that it was indeed a substrate and one with a K_m value that is almost 3-fold lower than that of the parent α-glucosyl fluoride. This reduction in K_m is quite significant given that an increase in true affinity as a consequence of the substitution of the C-5 hydrogen by fluorine is unlikely. A more likely explanation is that the second step has been slowed substantially more than the first by the fluorine substitution, with an accumulation of intermediate resulting. This phenomenon leads to a lowering of the K_m value when the second step clearly is rate-limiting. Further, the lower K_m value made measurement of isotope effects upon k_{cat} possible. As seen in Table 4, a very large α-deuterium kinetic isotope effect of $k_H/k_D = 1.23$ was observed for this substrate, consistent with fully developed oxocarbenium ion character at the transitioin state. In this case, however, a substantial isotope effect of $k_H/k_D = 1.92$ was seen for the 2-deutero substrate. This value is clearly outside the range of a β-secondary isotope effect and within the range of a primary kinetic isotope effect. This therefore provides the first direct kinetic proof of a two-step mechanism for which the second step involves at least partially rate-limiting C−H bond cleavage. This primary KIE is relatively small for the E2 mechanism, while the KIE measured with the 1-deutero derivative is quite large for an α-secondary deuterium KIE. On the basis of this pair of values, some distinction can be made between stepwise and concerted mechanisms for the elimination. First of all, the carbanion mechanism (E1cB) can be ruled out since large α-secondary isotope effects have never been measured for such a mechanism (*49*) and since, of course, the β-proton is not activated. The large secondary α-KIE might on its own indicate an E1 mechanism, but the presence of a primary KIE at C2 eliminates a fully stepwise E1 mechanism. An E1 mechanism involving anchimeric assistance by the β-hydrogen and nucleophilic attack of solvent on the β-hydrogen has been previously shown to yield small primary KIE values of 1.72∼1.85 (*50*). However, such a mechanism is not likely in this case since the β-hydrogen is located on the same face of the pyranose ring as the scissile bond. A concerted mechanism with an asymmetric transition state involving extensive cleavage of the glycosidic bond and substantial proton transfer is more probable and consistent with oxocarbenium ion chemistry. A small primary KIE may mean that the proton is either less than half or more than half transferred at the transition state. The latter case is inconsistent with substantial positive charge at the anomeric center. Thus, delayed proton transfer seems more probable. Indeed, a mechanism in which substantial heterolysis of the glycosidic bond occurs will generate a species with highly developed oxocarbenium ion character, thereby acidifying the β-hydrogen to be transferred. The E2 mechanism is not necessarily completely synchronous, and there can be a broad spectrum of transition states from carbocation-like to completely synchronous to carbanion-like in the E2 mechanism,

as excellently depicted by the potential energy surface diagrams of More O'Ferrall (*51*). Such an E2 mechanism leaning toward E1 was previously invoked to explain low KIE values (2.4∼2.6) of some nonenzymatic E2 reactions (*52*). Further, a similar kind of E1 type E2 enzymatic syn-elimination was found in UDP-*N*-acetylglucosamine 2-epimerase, where a primary KIE of 1.8 was measured (*53*).

These data combine to provide substantial evidence for a two-step mechanism via transition states with highly developed oxocarbenium ion character. One additional approach to probe charge development involves the measurement of effects of fluorine substitution adjacent to the reaction center upon reaction rates. As can be seen from Table 3, the effects of substitution of a second fluorine at C-1, C-2, and C-5 on rates of cleavage of αGlcF have been explored. Substitution at C-1 and C-5 involves replacement of H by F, which may cause very minor steric penalties but does not remove any potentially important hydrogen bonding interactions as is possibly the case at C-2. Further, substitution at C-2 and C-5 is adjacent to the developing oxocarbenium ion, whereas substitution at C-1 is directly on the carbocation. Previous solvolysis studies with 2-deoxy-2-fluorosugar derivatives have revealed an approximately 60-fold rate reduction as a consequence of such a substitution (*54*). Effects of substitution right at the cationic center are less predictable. Indeed, a stabilizing effect by lone pairs on fluorine substituted directly on carbocations has been seen (*55*), although studies of spontaneous solvolysis of **5** have revealed substantial rate reductions corresponding to an increase of free energy of activation ($\Delta\Delta G^{\ddagger}$) of 18.5 kJ mol^{-1} (*29*). The difference in behavior presumably resides in the oxocarbenium ion character in this case: lone pair donation by the oxygen totally dominates any possible donation by fluorine, leaving only the destabilizing inductive effect. Interestingly, $\Delta\Delta G^{\ddagger}$ values for all three substitutions on the enzymatic reaction were approximately 20 kJ mol^{-1} and thus very similar to that seen for spontaneous solvolysis. Since the nonenzymatic process has been shown to involve substantial carbocationic character (*56*, *57*), a similar transition state is predicted for the enzymatic process. An intriguing additional possible outcome for the reaction of **5** with GLase was a time-dependent inactivation due to the accumulation of a 2-keto glucosyl−enzyme intermediate. This could have arisen if the initially formed 1-fluoro-*β*-glucosyl enzyme had undergone a 1,2-trans-elimination of HF to yield an enolic glycosyl enzyme that would then ketonize. The fact that this otherwise chemically preferred trans-elimination did not occur is suggestive of a finely tuned and optimized enzymatic syn-elimination process.

Conclusion. On the basis of our initial accounts and present findings, the mechanism of GLase is suggested to be as depicted in Scheme 3, which is highly similar in many aspects to that of α-glucosidases of glycoside hydrolase family 31. Such a mechanism involves the formation and base-catalyzed elimination of a covalent glycosyl−enzyme intermediate. The glycosyl−enzyme intermediate is formed through a transition state with significant oxocarbenium ion character in which the carbon−oxygen bond is broken substantially, but the negative charge on the leaving group oxygen is largely masked by advanced proton donation by the acid/base catalyst. The covalent intermediate so formed then undergoes an elimination reaction that follows an E1-like E2 mechanism via a transition state in which the C−O bond at the anomeric center is largely broken and the anomeric center assumes substantial oxocarbenium ion character. The oxocarbenium ion character of this species leads to substantial acidification of the C-2 proton allowing its relatively facile removal. The identity of the base responsible for H-2 abstraction is not clear at this stage. However, a very strong candidate for this role must be the departing carboxylate oxygen of the catalytic nucleophile itself (Asp 553). This group is correctly positioned on the *β*-face of the sugar, and since the transition state is late, will be available to act as a base. Indeed, three-dimensional structures of intermediates trapped on other α-glycosidases and transglucosidases (ref *58* and David Rose, personal communication) reveal that the carbonyl oxygen of the nucleophile is situated in close proximity to the endocyclic oxygen of the sugar ring. A small rotation around the C−O bond would suffice to place the oxygen correctly to act in this role. Additional support for this notion comes from the observation that retaining glycosidases catalyze the hydration of glycal substrates via a covalent glycosyl−enzyme intermediate and do so via the syn-addition of the proton at C-2 and the enzymic nucleophile. It has been generally assumed that the nucleophile itself donates this proton in a somewhat concerted process highly analogous to that proposed for GLase (*18*). In addition, Wolfenden earlier noted that the ribosylation reaction catalyzed by nucleoside 2-deoxyribosyltransferase is accompanied by the occasional elimination reaction, generating D-ribal (*59*). This also points to the existence of a mechanistic continuum. This is a novel mechanism for glycosidic bond cleavage but one in which

Scheme 3: Proposed Mechanism of α-1,4-Glucan Lyase[a]

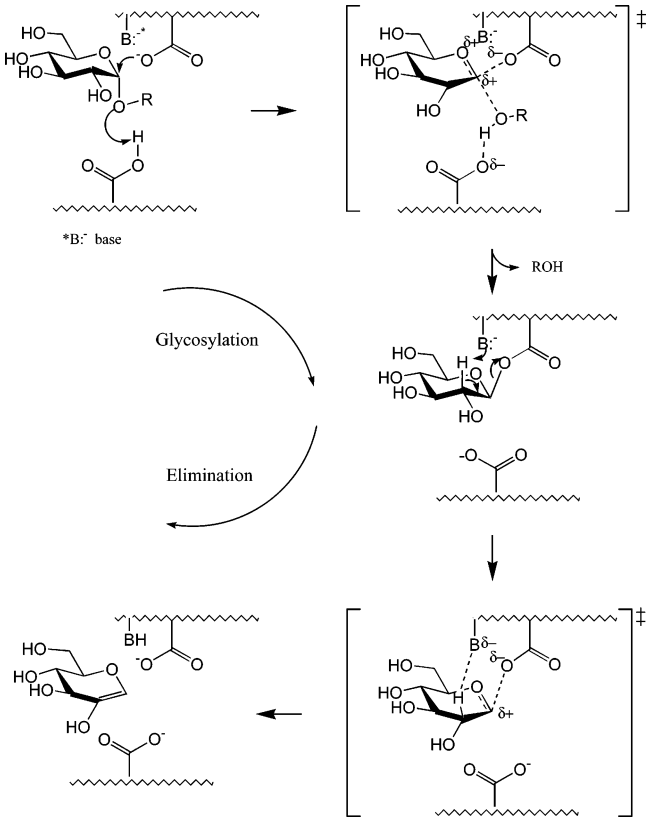

[a] Present findings are reflected in the depiction of both transition states.

all processes except the second step are common aspects of α-glucosidases of family 31, leading to the idea that GLase utilizes mechanistic machinery that is common to family 31. It therefore represents an example of a way in which enzymatic mechanisms can evolve through subtle changes in active site constitution. These results firmly illustrate that GLase does not follow the chemistry of other enzymes that catalyze β-elimination but complies to the chemistry inferred by the amino acid sequence homology. These commonalities highlight the advantages of the sequence-based classification of glycosidases in considering reaction mechanisms and provide further caution about the annotation of genomes purely on the bases of sequence similarity.

REFERENCES

1. Sinnott, M. L. (1990) *Chem. Rev. 90*, 1171−1202.
2. McCarter, J. D., and Withers, S. G. (1994) *Curr. Opin. Struct. Biol. 4*, 885−892.
3. Zechel, D. L., and Withers, S. G. (2000) *Acc. Chem. Res. 33*, 11−18.
4. Henrissat, B. (1991) *Biochem. J. 280*, 309−316.
5. Henrissat, B., and Bairoch, A. (1993) *Biochem. J. 293*, 781−788.
6. Henrissat, B., and Davies, G. J. (2000) *Plant Physiol. 124*, 1515−1519.
7. Ernst, S., Langer, R., Cooney, C. L., and Sasisekharan, R. (1995) *Crit. Rev. Biochem. Mol. Biol. 30*, 387−444.
8. Rye, C. S., and Withers, S. G. (2002) *J. Am. Chem. Soc. 124*, 9756−9767.
9. Yu, S., Bojsen, K., Svensson, B., and Marcussen, J. (1999) *Biochim. Biophys. Acta 1433*, 1−15.
10. Yu, S., Kenne, L., and Pedersén, M. (1993) *Biochim. Biophys. Acta 1156*, 313−320.
11. Yu, S., and Pedersén, M. (1993) *Planta 191*, 137−142.
12. Yu, S., Ahmad, T., Kenne, L., and Pedersén, M. (1995) *Biochim. Biophys. Acta 1244*, 1−9.
13. Yu, S., Christensen, T. M. I. E., Kragh, K. M., Bojsen, K., and Marcussen, J. (1997) *Biochim. Biophys. Acta 1339*, 311−320.
14. Kametani, S., Shiga, Y., and Akanuma, H. (1996) *Eur. J. Biochem. 242*, 832−838.
15. Shiga, Y., Kametani, S., Kadokura, T., and Akanuma, H. (1999) *J. Biochem. 125*, 166−172.
16. Bojsen, K., Yu, S., Kragh, K. M., and Marcussen, J. (1999) *Biochim. Biophys. Acta 1430*, 396−402.
17. Bojsen, K., Yu, S., and Marcussen, J. (1999) *Plant Mol. Biol. 40*, 445−454.
18. Legler, G. (1990) *Adv. Carbohydr. Chem. Biochem. 48*, 319−384.
19. Yoshinaga, K., Fujisue, M., Abe, J., Hanashiro, I., Takeda, Y., Muroya, K., and Hizukuri, S. (1999) *Biochim. Biophys. Acta 1472*, 447−454.
20. Nyvall, P., Pedersén, M., Kenne, L., and Gacesa, P. (2000) *Phytochemistry 54*, 139−145.
21. Quaroni, A., and Semenza, G. (1976) *J. Biol. Chem. 251*, 3250−3253.
22. Hermans, M. M. P., Kroos, M. A., van Beeumen, J., Oostra, B. A., and Reuser, A. J. J. (1991) *J. Biol. Chem. 266*, 13507−13512.
23. Iwanami, S., Matsui, H., Kimura, A., Ito, H., Mori, H., Honma, M., and Chiba, S. (1995) *Biosci. Biotech. Biochem. 59*, 459−463.
24. Kimura A., Takaya M., Fukushi Y., Mori, H., Matsui, H., and Chiba, S. (1997) *Biosci. Biotech. Biochem. 61*, 1091−1098.
25. Lee, S. S., He, S., and Withers, S. G. (2001) *Biochem. J. 359*, 381−386.
26. Lee, S. S., Yu, S., and Withers, S. G. (2002) *J. Am. Chem. Soc. 124*, 4948−4949.
27. Cogoli, A., and Semenza, G. (1975) *J. Biol. Chem. 250*, 7802−7809.
28. Igaki, S., and Chiba, S. (1989) *Abstracts of the Annual Meeting of the Japan Agricultural Society, Niigata, Japan*, 3Hp16, p 292, Agricultural Chemical Society of Japan, Tokyo.
29. Konstantinidis, A., and Sinnott, M. L. (1991) *Biochem. J. 279*, 587−593.
30. Praly, J.-P., and Descotes, G. (1987) *Tetrahedron Lett. 28*, 1405−1408.
31. Adamson, J., Foster, A. B., Hall, L. D., Johnson, R. N., and Hesse, R. M. (1970) *Carbohydr. Res. 15*, 351−359.
32. McCarter, J. D., and Withers, S. G. (1996) *J. Am. Chem. Soc. 118*, 241−242.
33. Hayashi, M., Hashimoto, S., and Noyori, R. (1984) *Chem. Lett.* 1747−1750.
34. Wolfrom, M. L., and Thompson, A. (1963) *Methods Carbohydr. Chem. 2*, 211−215.
35. Kooners, H. J., de Kok, A. J., Romers, C., and van Boom, J. H. (1980) *Recl. Trav. Chim. Pays-Bas 99*, 355−362.
36. Yamaguchi, M., Horiguchi, A., Fukuda, A., and Minami, T. (1990) *J. Chem. Soc., Perkin Trans. 1*, 1079−1082.
37. Apparu, M., Blanc-Muesser, M., Defaye, J., and Driguez, H. (1981) *Can. J. Chem. 59*, 314−320.
38. Farkas, I., Szabo, I. F., and Bognar, R. (1976) *Carbohydr. Res.* 48, 136−138.
39. Joshi, M. D., Sidhu, G., Pot, I., Brayer, G. D., Withers, S. G., and McIntosh, L. P. (2000) *J. Mol. Biol. 299*, 255−279.
40. McCarter, J. D., and Withers, S. G. (1996) *J. Biol. Chem. 271*, 6889−6894.
41. Kimura, A., Somoto, A., Mori, H., Sakai, O., Matsui, H., and Chiba, S. (1997) *Biosci. Biotech. Biochem. 61*, 475−479.
42. Kempton, J. B., and Withers, S. G. (1992) *Biochemistry 31*, 9961−9969.
43. Vocadlo, D. J., Wicki, J., Rupitz, K., and Withers, S. G. (2002) *Biochemistry 41*, 9727−9735.
44. Tull, D., and Withers, S. G. (1994) *Biochemistry 33*, 6363−6370.
45. Mosi, R., Sham, H., Uitdehaag, J. C. M., Ruiterkamp, R., Dijkstra, B. W., and Withers, S. G. (1998) *Biochemistry 37*, 17192−17198.
46. Hoos, R., Vasella, A., Rupitz, K., and Withers, S. G. (1997) *Carbohydr. Res. 298*, 291−298.
47. Heightman, T. D., and Vasella, A. T. (1999) *Angew. Chem., Int. Ed. Engl. 38*, 750−770.
48. Williams, S. J., Hoos, R., and Withers, S. G. (2000) *J. Am. Chem. Soc. 122*, 2223−2235.
49. Fry, A. (1972) *Chem. Soc. Rev. 1*, 163−210.
50. Cram, D. J., and Tadanier, J. (1959) *J. Am. Chem. Soc. 81*, 2737−2748.
51. More O'Ferrall, R. A. (1970) *J. Chem. Soc. B*, 274−277.
52. Bunnet, J. F., Davis, G. T., and Tanida, H. (1962) *J. Am. Chem. Soc. 84*, 1606−1614.
53. Morgan, P. M., Sala, R. F., and Tanner, M. E. (1997) *J. Am. Chem. Soc. 119*, 10269−10277.
54. Withers, S. G., MacLennan, D. J., and Street, I. P. (1986) *Carbohydr. Res. 154*, 127−144.
55. Blint, R. J., McMahon, T. B., and Beauchamp, J. L. (1974) *J. Am. Chem. Soc. 96*, 1269−1278.
56. Sinnott, M. L., and Jencks, W. P. (1980) *J. Am. Chem. Soc. 102*, 2026−2032.
57. Banait, N. S., and Jencks, W. P. (1991) *J. Am. Chem. Soc. 113*, 7958−7963.
58. Uitdehaag, J. C. M., Mosi, R., Kalk, K. H., van der Veen, B. A., Dijkhuizen, L., Withers, S. G., and Dijkstra, B. W. (1999) *Nat. Struct. Biol. 6*, 432−436.
59. Smar, M., Short, S. A., and Wolfenden, R. (1991) *Biochemistry 30*, 7908−7912.

BI035189G